


 Cite this: *Sens. Diagn.*, 2024, 3, 1392

## Optimization of solvents, electrolytes, and mediators for polyindole-based electrochemical sensors

 P. C. Pandey, \*<sup>a</sup> Atul Kumar Tiwari <sup>a</sup> and Roger J. Narayan \*<sup>b</sup>

Surface-engineered conducting polymers (CPs) have enabled technological advances in chemistry and materials science. Heterocyclic conjugated organic molecules, specifically indole and its derivatives, have the potential to be polymerized under electrochemically controlled conditions in different types of compatible solvent media, including self-assembled nanofluids, for several applications. Polymer-based electrode materials are valuable for the detection of various targeted biomolecules and other analytes. This review outlines the evolution of the electropolymerization technique in recent years, along with developments in the field. With advances in nanoscience, several materials have been used to modify CPs for electrochemical sensing. Several biomedical applications and the role of antifouling agents in the properties of several electropolymerized thin films are highlighted.

 Received 28th May 2024,  
 Accepted 26th July 2024

DOI: 10.1039/d4sd00175c

[rsc.li/sensors](https://rsc.li/sensors)

### 1. Introduction

Over the past several decades, electropolymerization has emerged as a promising tool for designing new functional sensors.<sup>1–5</sup> Electrochemical conversion and deposition of aromatic monomers into long-chain conducting polymers (CPs) at the electrode surface have demonstrated the role of delocalized systems in practical applications (Chart 1).<sup>1,6</sup> Applications ranging from defensive cladding to highly selective biosensors have benefitted from the use of electrochemically responsive polymer films.<sup>4–11</sup> Organic polymers exhibit an insulating nature in the neutral state; upon doping with redox agents, they are favorably transformed into electroactive polymers.<sup>12,13</sup> Many investigations on the electron hopping behavior and charge transport mechanisms, along with investigations on chain length, have acknowledged the role of these materials as synthetic metals.<sup>13–15</sup> This concept led to the successful development of CPs using conjugated organic monomers.<sup>9,13</sup> In particular, heterocyclic compounds such as indole and its derivatives (Scheme 1) demonstrated exceptional properties in polymerization<sup>5–23</sup> due to structural delocalization (Scheme 2), enabling the formation of a variety of polymeric microstructures. Compared to other conducting polymers (e.g., PANI), PIN exhibits slower hydrolytic degradation and enhanced thermal stability. Moreover, PIN exhibits a more

competitive redox potential than PPY.<sup>24</sup> It also exhibits excellent photoluminescence properties,<sup>25</sup> stable redox activity,<sup>26</sup> low cost,<sup>27</sup> ease of synthesis,<sup>28</sup> fast switchable electrochromic properties,<sup>29</sup> air-stable electrical conductivity in the doped state,<sup>30</sup> and increased internal conductivity,<sup>31</sup> especially when utilized in energy storage device applications. However, the polymerization efficiency and the conductivity of polyindole are lower than those of other conducting polymers,<sup>32</sup> which has limited their evaluation by the research community compared to other conducting materials. It should be noted that the development of various types of composites and copolymers based on polyindoles and their derivatives has increased in recent years. At this time, more than twenty indole derivatives have been discovered (Scheme 1).<sup>6</sup> These polyindole derivatives, which are obtained through the polymerization of indole derivatives, exhibit

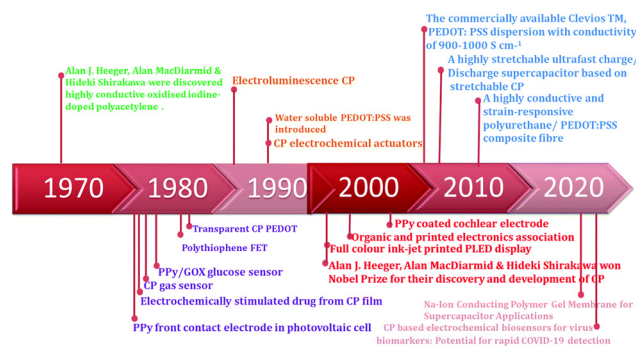
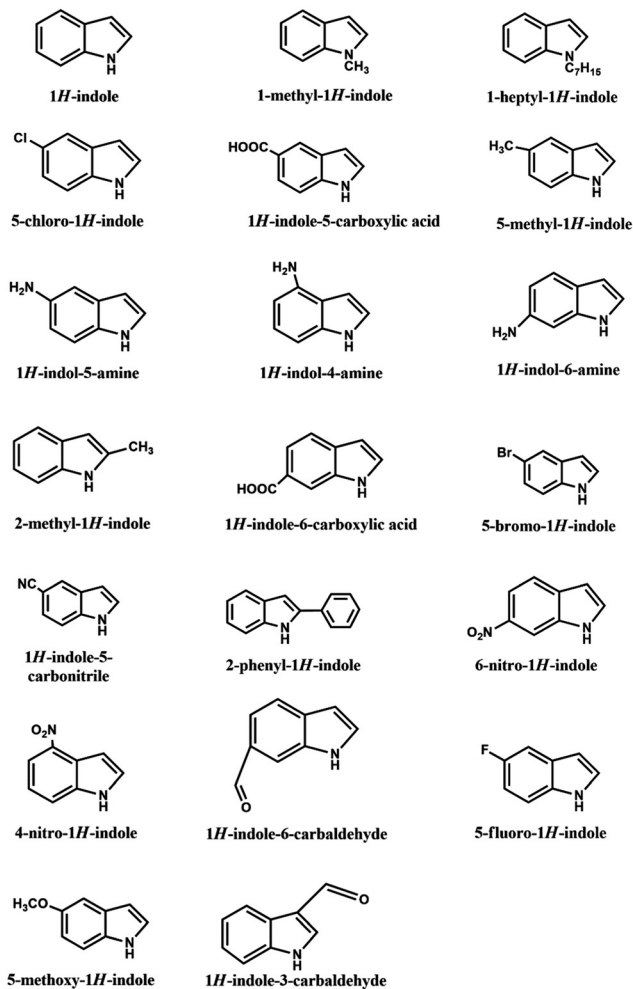


**Chart 1** Brief history of conducting polymers and their applications. Adapted with permission<sup>6</sup> © the authors.

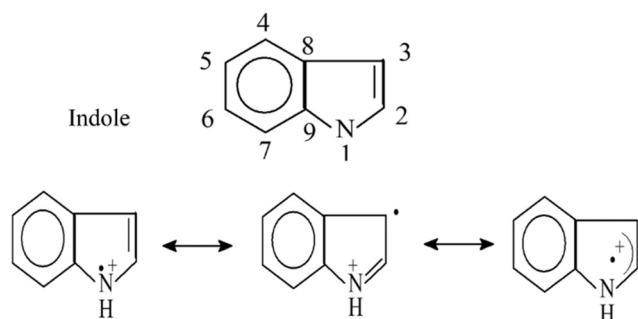
<sup>a</sup> Department of Chemistry, Indian Institute of Technology (BHU), Varanasi-221005, India. E-mail: pcpandey.apc@iitbhu.ac.in, atulkumartiwari.rs.chy19@iitbhu.ac.in

<sup>b</sup> Joint Department of Biomedical Engineering, University of North Carolina, Chapel Hill, NC, 27599, USA. E-mail: rjnaraya@ncsu.edu





Scheme 1 Indole and their derivatives.



Scheme 2 Structure of indole and electronic delocalization.

unique properties such as enhanced conductivity, photoluminescence, and redox activity. There are several methods for synthesizing PIN, including emulsion polymerization, oxidative polymerization, electrochemical polymerization, and interfacial polymerization.<sup>6</sup> Because of their high chemical and mechanical stability, relatively low cost, solvent adaptability, and ease of preparation, indole and substituted indoles have enabled the formation of excitable hydrophobic materials for water-soluble polymers.<sup>6</sup>

The fabrication of conducting polymer components is one of the most important requirements for conducting polymers; it is determined by the behavior and interactions of polymers with fillers, oils, redox materials, nanoparticles, and nanomaterials that may undergo interactions during the processing of polymeric domains for several applications. Indole is a potent heterocyclic monomer that is considered an intercellular signaling moiety that regulates several physiological processes, such as plasmid stability, spore formation, drug resistance, biofilm formation, and virulence. In addition, the amino acid derivative (*e.g.*, heterocyclic tryptophan) is a fluorescent indole derivative and precursor of serotonin, a neurotransmitter that controls a variety of vital metabolic processes through functionalities linked to the indole residue. Accordingly, the substituents present at positions 2, 3, 5, and 6 of the indole residue drastically alter the physicochemical properties of this heterocyclic monomer. Innovative polymerization protocols enable the processing of polymeric domains that are suitable for several applications.<sup>15–23,33</sup>

Furthermore, polymers derived from organic monomers and their composites have attracted interest owing to their unusual optical, electrical, mechanical, and thermal characteristics, which are associated with *in situ* polymer-nanoparticle interactions as well as the state of dispersion. The use of similar nanomaterials as electrode modifier materials and the ability of these nanomaterials to mediate electron transfer reactions in electroactive molecules have been well documented.<sup>34–56</sup> The use of functional nanoparticles as an initial modifier can lead to increased sensitivity by increasing the surface area of the electrode surface. Efforts have been made to utilize available nanomaterials, including nanoparticles,<sup>34</sup> multiwalled carbon nanotubes, quantum dots, graphene quantum dots, palladium nanoparticles, gold nanowires, and gold nanoparticles. In general, nanomaterials can enhance the sensitivity of CPs.<sup>22,35–46</sup> This approach has been used for different analytes, including novel biomarkers. In addition, commercial efforts have demonstrated the ability to miniaturize conducting polymer-based electrochemical devices containing homogenous suspensions of CP formulations. The siloxane polymer exhibits unusual properties because of the –Si–O–Si– unit of the polymer backbone,<sup>18,19,57–59</sup> which can be used to create self-assembled polyindole–siloxane nanofluids<sup>18–21</sup> for a variety of electrochemical sensor designs.<sup>20,21</sup>

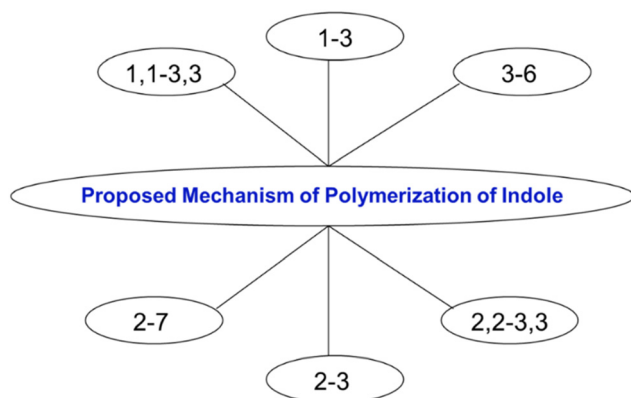
## 2. Electro-polymerization of heteroaromatic molecules: fundamentals of polyindole

Conjugated organic molecules (*e.g.*, pyrrole, thiophene, furan, indole, and carbazole) with heteroatoms (*e.g.*, N, O, and S) exhibit interesting electrical properties upon

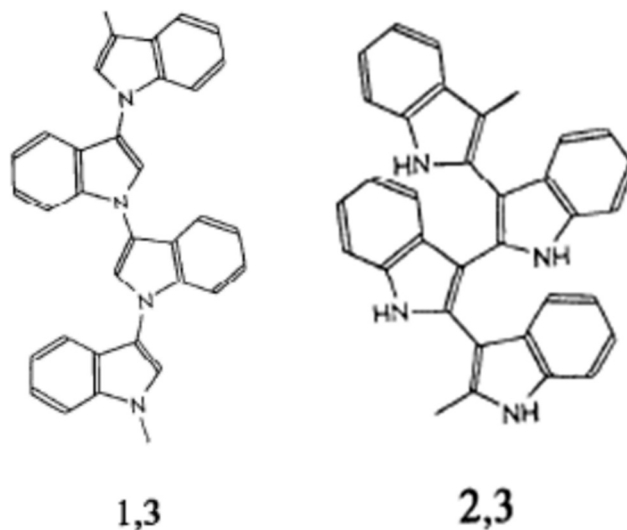


## Critical review

polymerization.<sup>47</sup> The electrochemically controlled oxidation of these aromatic molecules yields a thin film of CPs on the electrode surface. The conductivity of these polymeric materials is a function of electron delocalization along the chain length and dopant level.<sup>56</sup> Among the various polymers derived from heterocyclic monomers, polyindole (PIN) and its derivatives have potential uses in various applications, including electrochemical sensing, energy storage, and electrorheology.<sup>5,6,56</sup> Furthermore, the characteristics of the material can be controlled by modifying the different functional groups on the benzene ring because of the efficient tuning of the electronic delocalization between the heterocyclic ring and the benzene ring (Scheme 3). The electropolymerization of indole, which was first reported by Waltman *et al.*,<sup>5</sup> has attracted significant attention. Electropolymerized polyindoles, which exhibit various options in terms of radical cation propagation and termination,<sup>5,8</sup> were described for use in chemical sensors for glucose detection for the first time by Pandey *et al.*<sup>7</sup> The dependence of the polymerization process on the solvent, supporting electrolyte, and polymerization conditions allows for innovative approaches such as better adaptation to elevated temperatures and coordinated oxidation-reduction.<sup>7-9</sup> This material has been utilized in several applications, such as modified electrodes, redox capacitors, chemical sensors, and rechargeable batteries.<sup>7-19</sup> Tuning radical cation propagation and termination by controlling the solvent, supporting electrolyte, and even the monomer itself leads to a highly hydrophobic polyindole with excellent electrochromism for use as a potential material in rechargeable batteries.<sup>8</sup> Various experimental conditions, particularly the solvent used during the electropolymerization of indole, are important parameters; the water content in organic solvents controls the polymerization process.<sup>19</sup> It has been indicated that the formation of the polymer occurs through the 1-3 positions of the indole or the 2-3 positions of the heterocyclic residue (Schemes 4 and 5);<sup>60</sup> precise control of the propagation of the chain length of the polyindole due to steric hindrance (Scheme 3) is possible *via*



**Scheme 3** Probability of various available positions in indole for the radical cation position.

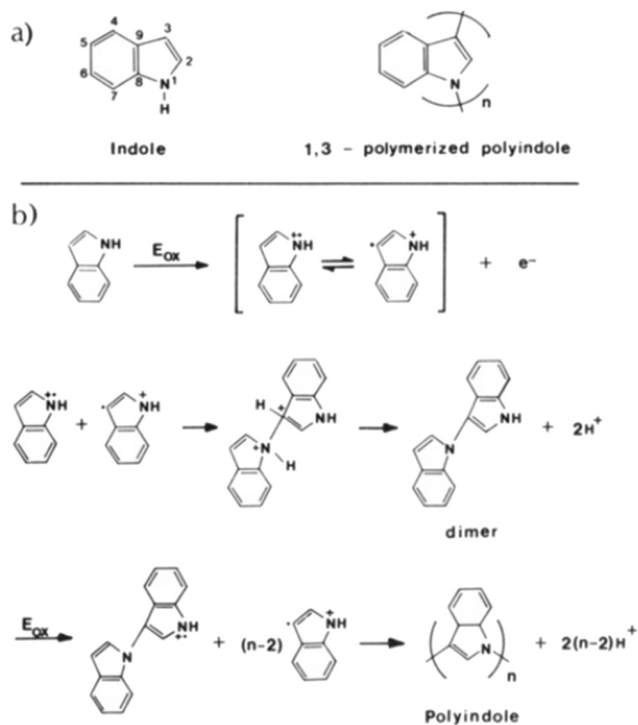


**Scheme 4** Dependence of radical cation propagation *via* only 1-3 and 2-3 positions of indole and expected steric hindrance.

this approach. These alternatives contribute to variations in the polymeric morphology, hydrophobicity, and electrochromism.

### 2.1 Factors controlling electro-polymerization of indole and indole derivatives

The performance of electrodeposited CPs depends on various conditions such as the solvents used (*e.g.*, aqueous/non-



**Scheme 5** Mechanism of electro-polymerization of indole; (a), polymerized form and (b) mechanism of polymerization. Reproduced with permission<sup>60</sup> © 1992 American Chemical Society.



aqueous), supporting electrolytes, and temperature.<sup>51–53</sup> Different combinations of solvents and electrolyte systems define the properties of the as-synthesized polymer films (as noted by Namsheer *et al.*).<sup>46</sup> Indole and its derivatives were first electropolymerized in acetonitrile; this procedure was reproducible and associated with a high yield.<sup>5</sup> Furthermore, polymerization was investigated in dichloromethane and an aqueous medium.<sup>8</sup> The presence of moisture in the solvent/supporting electrolyte/indole monomer is believed to lower the onset potentials for the process and chain propagation, drastically affecting the hydrophobicity and electrochromism of polyindole.<sup>8</sup> Boron trifluoride ethyl ether (BFEE), perchlorate ( $\text{LiClO}_4$ ), and acetonitrile (ACN) are suitable ionic solvents for the process. Tetraphenylborate (TPB), tetraethylammonium tetrafluoroborate (TETFB), tetramethylammonium perchlorate (TMAP), BFEE, and  $\text{LiClO}_4$  are suitable supporting electrolytes for the process.<sup>36–40</sup> When utilized along with other organic solvents, acids generate conducting species that maintain ionic conductivity. The typical polymerization growth of conducting polyindoles from indole and its carboxylic acid, <sup>15–17</sup> especially indole-5-carboxylic acid (I5CA) and indole-6-carboxylic acid (I6CA), is described in Fig. 1. The

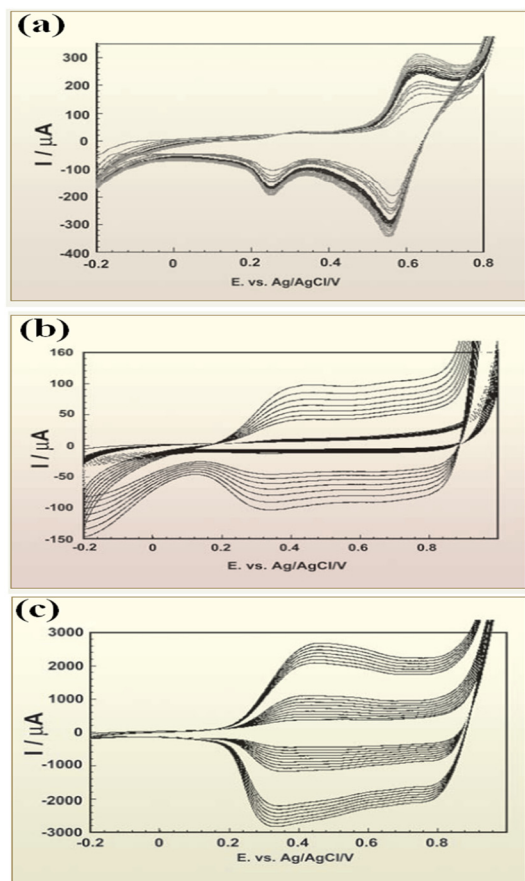


Fig. 1 Potentiodynamic electro-polymerization of (a) indole, (b) I5CA, and (c) I6CA in 0.1 M tetrabutylammonium perchlorate solution. Adopted with permission from ref. 15.

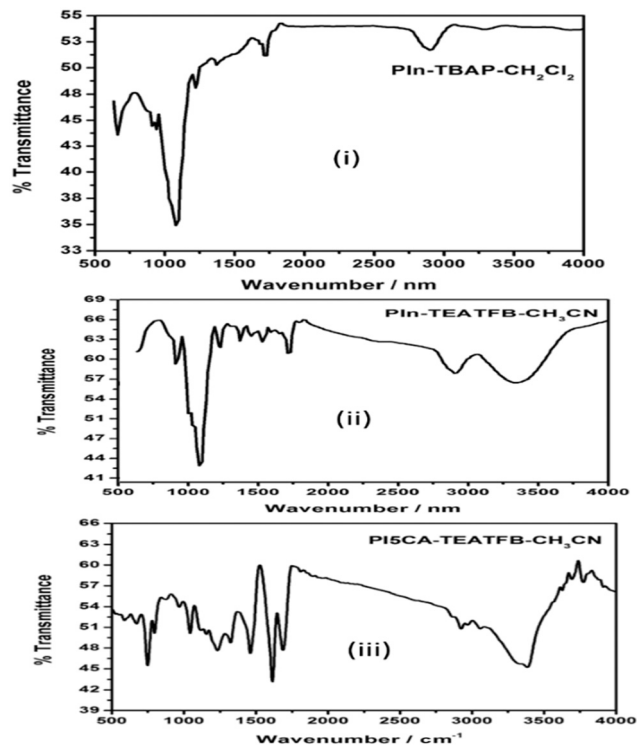


Fig. 2 FTIR of polyindole made in dichloromethane (i) and acetonitrile (ii). FTIR of polyindole made from indole-5-carboxylic acid in the presence of 0.1 MTBAP and TEATFB (iii).

properties of the polymers obtained from FTIR and XRD are shown in Fig. 2 and 3, respectively, which indicate the dependence of the material properties on the solvent and supporting electrolytes. These findings indicate that the polymer prepared in dichloromethane was devoid of N–H stretching (Fig. 2(i)). The material displays excellent hydrophobicity with good electrochromic activity, and has potential for use in rechargeable battery applications.<sup>8</sup>

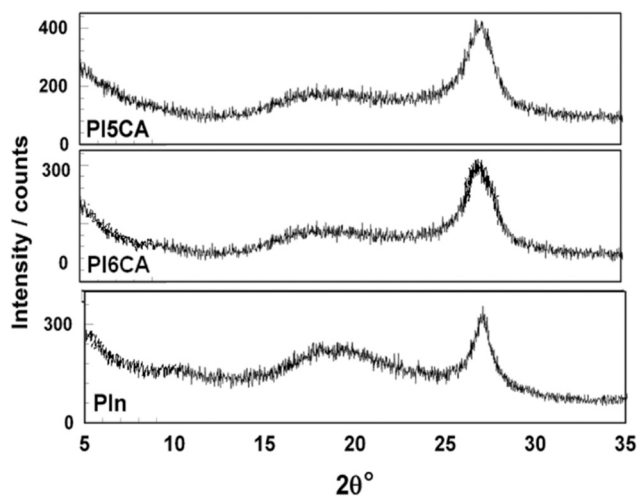


Fig. 3 XRD data from polyindole (PIN), poly(indole-5-carboxylic acid), as well as poly(indole-6-carboxylic acid).



Similarly, the crystallinity of polyindole was also shown to be of high quality when prepared in dichloromethane (Fig. 3).

The polyindole synthesized in mixed electrolyte systems has been noted to be of high quality. Indole is electrically polymerized under acidic conditions.<sup>52–55</sup> These systems involve both adsorption and electrodeposition, and the situation at the electrified interface has been evaluated *via* electrochemical studies such as cyclic voltammetry (CVs). Two non-aqueous solvents, acetonitrile and dichloromethane, along with the supporting electrolytes, TETFB and TMAP, were utilized for the process.<sup>47</sup> Solvents and electrolytes of varying polarities are often used to introduce polarity/non-polarity within indole moieties, and facilitate the formation of radical cations in this molecule. The solvent-to-electrolyte ratio is responsible for the overall growth of the polymer; the solubility of the monomer and supporting electrolyte in a particular solvent, the apparent solubility of radical cations in the respective solvent, and the presence of nucleophiles in the electro-polymerization medium in a specific solvent are important parameters. The higher solubility of both the monomer and supporting electrolyte supports the high yield of polymer formation.<sup>47–55</sup>

### 3. Recent developments in polyindole-based electrochemical sensors

Uniform electro-polymerized films of CPs, which are strongly adherent to the electrode surface, have been utilized to design various sensing systems in recent decades. The susceptibility to polymeric growth in an aqueous system with a polar organic solvent enabled the preparation of polyindole for use in glucose biosensing.<sup>7</sup> However, when polymer growth was allowed in an aprotic solvent with a dehydrated polymerizing agent, an excellent hydrophobic polymer exhibiting electrochromism was achieved.<sup>8</sup> Upon oxidation (doping), the hydrophobic polymer changed its color to khaki green. However, upon reduction, the polymer changed to a golden yellow color. Thus, there was a striking difference in color upon electrochemical perturbation in the hydrophobic polymer, making it superior to more common conducting polymers for applications in electrochromic devices and rechargeable batteries.<sup>8</sup> In addition, these polyindole electrodes can be easily manipulated by an ion exchanger, such as tetraphenylborate; they may be converted into solid-state non-specific anion-selective electrodes, with the possibility of being configured into PVC membrane-based selective ion-selective electrodes for cations by assembling a neutral carrier-impregnated PVC matrix membrane<sup>13,14</sup> over a polyindole/electrode. The redox activity of the polyindole film showed the selectivity characteristics of the neutral-carrier-based ion sensor.<sup>13</sup> The polymer electrode generated by the electropolymerization of the indole monomer in dichloromethane, which contained tetrabutylammonium perchlorate and tetraphenylborate, displayed excellent

characteristics as a solid-state ion-selective electrode for non-specific anions and served as an excellent polymer/electrode dipolar interface for neutral carrier-mediated solid-state cation ion sensing.<sup>13,14</sup> The resulting ion-selective electrode displayed an excellent reproducible potentiometric signal, with the lowest detection limit characteristics for a potassium ion sensor ( $7.0 \times 10^{-6}$  mol dm<sup>-3</sup>) and wide linearity.<sup>12–14</sup> Many other reports on polyindole-based electrochemical sensors for picric acid<sup>61</sup> and methanol<sup>62</sup> have also been documented, justifying the potential use of polyindole in a variety of electrochemical applications, including rechargeable batteries, supercapacitors, electrochemical sensors, and biosensors. Wang *et al.* reported the impact of introducing fluorine on the properties of polyindole thin films with high energy storage behavior, high specific capacitance values, and good cycle stability. The structure of the polyindole differed with the degree of fluorine substitution.<sup>53</sup>

#### 3.1 Polyindole as surface-modified chemical sensors

The capability for facile fabrication is a potential issue in CPs when preparing materials with a desired composition. Processing of hydrophobic polyindoles is difficult in any organic solvent; however, polyindoles prepared in acetonitrile can be easily dissolved in DMSO. The polymers made from I5CA and I6CA in acetonitrile were dissolved in DMSO, and the spectra are shown in Fig. 4. All of the polymers showed

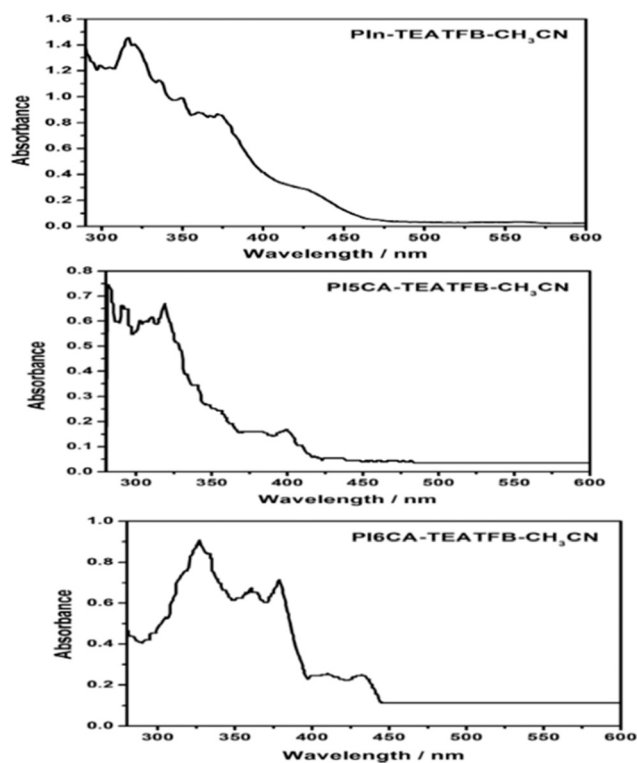


Fig. 4 UV-vis spectra of polyindole made from P5CA as PI5CA and I6CA as PI6CA in DMSO.



absorption in the UV range and visible range. The similarity in the spectra indicated the presence of similar basic polymeric unit patterns in the substituted and unsubstituted polyindoles. A broad absorption indicated a significant conjugation chain length in the polymeric domains; the absorption spectra confirmed the formation of polymers with longer polymer sequences. Electrochemical non-enzymatic sensors of CPs with elementary modifications (for instance, the addition of mediators) were effectively utilized for the detection of small molecules such as glucose, dopamine, ions, and hydrogen peroxide ( $\text{H}_2\text{O}_2$ )<sup>1-5,16-19,51-58</sup>-mediated bioelectrochemical reactions. Functional groups such as carboxylic acids present at the 5- and 6-positions of the indole residue undergo potentiodynamic polymerization in acetonitrile, yielding PI5CA and PI6CA, respectively; these materials are water-soluble polymers for a variety of applications,<sup>16,17</sup> displaying variable spectroscopic properties as a function of the substituent position in the indole residue (as shown in Fig. 5). The UV-vis spectra of soluble PI5CA and PI6CA were recorded in 10 mM Tris-HCl buffer (pH 7.0), as shown in Fig. 5. Fig. 5 was found to be very similar to that recorded in DMSO (Fig. 4). The absorption spectrum of PI6CA displayed a broad band with significant shoulder features at 259, 318, and 367 nm; fine structural features were observed at 351 nm. In contrast, PI5CA exhibited blue shifts at 230, 273, and 352 nm. PI6CA and PI5CA differed significantly in terms of their color when dissolved in Tris-HCl buffer; the photographs and spectra of the visible region are provided in Fig. 5. The absorption characteristic at a wavelength of 418 nm in the case of PI6CA shifted to a wavelength of 390 nm in the case of PI5CA. The blue shift

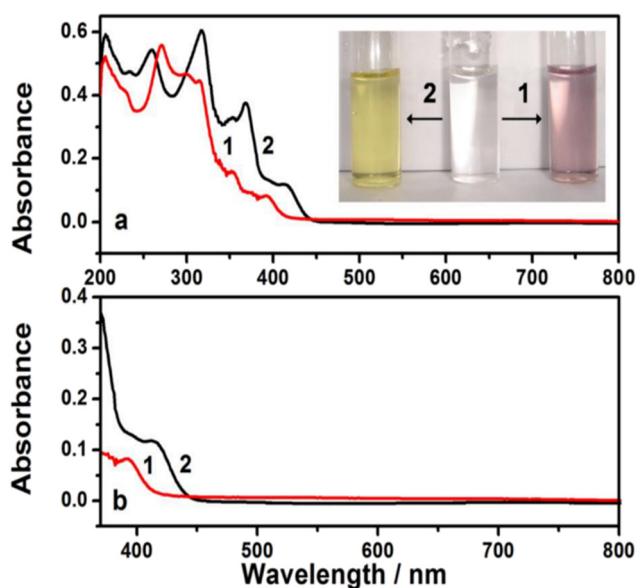


Fig. 5 (a) Absorption spectra of PI5CA (1) and PI6CA (2) in 10 mM Tris-HCl buffer (pH 7.0); (b) absorption spectra of PI5CA (1) and PI6CA (2) in 10 mM Tris-HCl buffer (pH 7.0). The inset showed the visual photographs of PI5CA (1) and PI6CA (2) dissolved in 10 mM Tris-HCl buffer (pH 7.0). Adopted with permission from ref. 23.

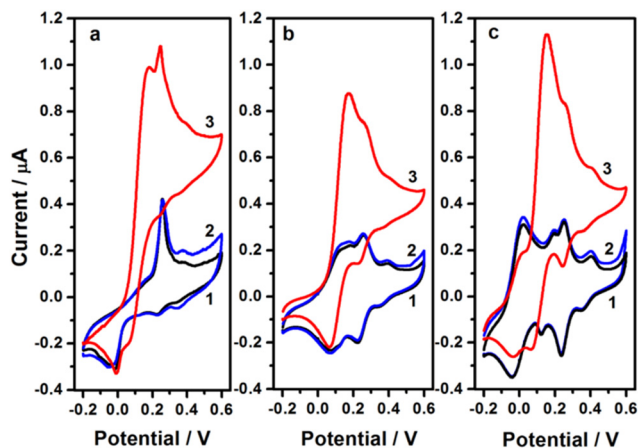


Fig. 6 Cyclic voltammograms of PI6CA modified containing (a) (1) TCNQ, (b) (1) Fc, and (c) (1) dmFc; (2) in the presence of 1 mM AA and (3) +0.1 mM DA in 100 mM phosphate buffer (pH 7.4) at the scan rate of  $0.01 \text{ V s}^{-1}$ . Adopted with permission from ref. 23.

noted in the UV absorption spectrum of PI5CA indicated either a shortening of the polymer chain length or a decrease in the level of conjugation.

Water-soluble PI5CA and PI6CA were explored for embedding redox mediators of organic metals, such as tetracyanoquinodimethane (TCNQ), ferrocene monocarboxylic acid (Fc), and dimethyl ferrocene (dmFc), to develop polymer-based electrochemical sensors.<sup>16</sup> PI5CA and PI6CA films were noted to be soluble in 10 mM Tris-HCl buffer (pH 7.0);  $0.2 \text{ mg mL}^{-1}$  solute of the material along with  $5 \mu\text{L}$  Nafion® alcoholic solution allowed the formation of a polymer-Nafion®-modified electrode. To enable doping of the electrode, tetracyanoquinodimethane (TCNQ), dimethyl ferrocene (dmFc), and ferrocene (Fc), which are well-known redox mediators for a variety of enzymatic and electroactive analyte-dependent bioelectrochemistry applications, were introduced into the polymer domain. The dried polymer-

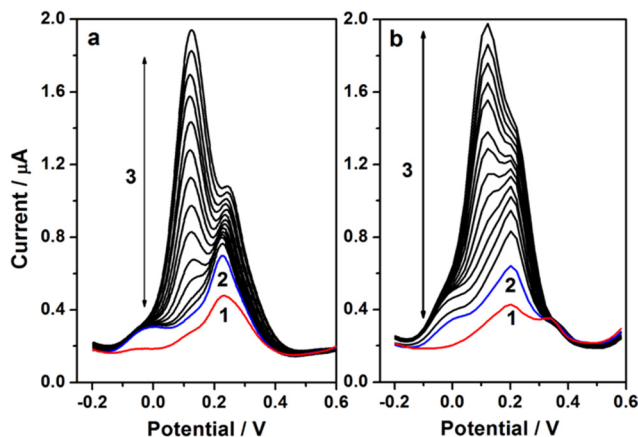


Fig. 7 Differential pulse voltammograms of a polymer-modified electrode that was made with w (a) (1) PI5CA and (b) (1) PI6CA, (2) containing 1 mM AA, (3) with the repeated addition of DA from 0.1 mM to 0.1 mM in 100 mM phosphate buffer (pH 7.4). Adopted with permission from ref. 23.



modified electrodes were used for electroanalysis of dopamine (DA) in the presence of ascorbic acid (AA), as shown in Fig. 6.<sup>16</sup> Redox mediators and polymer-modified electrodes were examined for dopamine sensing. The results shown in Fig. 6 justify the excellent mediated bioelectrochemistry as a function of dopamine concentration, without significant interference in the presence of the maximum biological concentration of ascorbic acid<sup>16</sup> (based on DPV responses) (Fig. 7). These results indicate that the incorporation of the three electron transfer mediators explains the electrochemical response upon the addition of DA. Furthermore, among the three electron transfer mediators utilized in this study, the contribution of TCNQ to the signal amplification of DA oxidation was found to be much better in the polymer-modified electrode<sup>16</sup> in terms of sensitivity and selectivity in the absence of a redox mediator, as shown in Fig. 8. These findings demonstrate the potential of the polyindole-modified electrode for electrochemical sensing applications.

### 3.2 Polymer-nanomaterial modified electrochemical sensors

Efforts are being made to enhance the activity of CPs by modifying them with various electroactive and catalytic nanomaterials such as graphene derivatives, organically modified silicates (Ormosil®), metal nanoparticles, and single- and multi-walled carbon nanotubes for use as efficient electrochemical sensors/biosensors.<sup>25</sup> One potential nanostructured matrix is organically modified silicates derived from organotrialkoxysilane<sup>63–65</sup> via sol-gel processing. Accordingly, soluble polyindole, along with gold nanoparticles (AuNPs) and silver nanoparticles (AgNPs), can be easily incorporated within an Ormosil film that is cast over the targeted electrode surface; the electrochemical responses to the selective analytes can be manipulated from these nanomaterials along with the polymeric indole

constituent. Therefore, we chose to incorporate silver and gold nanoparticles into Ormosil films together with soluble indole and potassium ferricyanide, which serve as efficient electron transfer redox mediators.<sup>17,22</sup> Three Ormosil® films, as shown in Fig. 9, were prepared by encapsulating potassium ferricyanide and PI6CA in the absence of metal nanoparticles (Ormosil®-1), in the presence of silver nanoparticles (Ormosil®-2), and in the presence of AuNPs (Ormosil®-3); the electrochemical oxidation of dopamine was evaluated in the presence of physiological concentrations of ascorbic acid<sup>17</sup> (Fig. 9).

Cyclic voltammograms of the bare Ormosil electrode are shown in curve 1 in Fig. 9; curves 2 and 3 show the same response towards 1 mM of AA and 20 M of DA, respectively. These voltammograms (Fig. 9) indicate the redox couple characteristics of potassium ferricyanide for oxidation as well as the reduction peak potentials of ferricyanide for Ormosil®-1 at 0.34 V and 0.17 V, for Ormosil-2 at 0.32 V and 0.22 V, and for Ormosil®-3 at 0.31 V and 0.23 V, respectively. The results shown in Fig. 9 suggest that ferricyanide within the Ormosil® matrix enabled electrocatalytic activity during DA oxidation. A significant decrease in the oxidation–reduction peak potential separation for Ormosil-2 and Ormosil-3 justified the contribution of noble metal nanoparticles during the oxidation of DA in comparison to that of bare Ormosil-1 (made without NPs). In addition, the sensitivity of DA analysis was improved compared to that of Ormosil-1 and the modified electrode processed with hydrophobic redox mediators (Fig. 7 and 8). Fig. 10 Shows typical DPV responses for Ormosil-1 (Fig. 10a), Ormosil-2 (Fig. 10b), and Ormosil-3 (Fig. 10c) in the presence of several DA concentrations. The concentration of AA was maintained at a constant value (1 mM); oxidation of DA at values of 0.23 V for Ormosil-1, 0.22 V for Ormosil-2, and 0.2 V for Ormosil-3 was demonstrated. The sensitivity towards DA detection was  $54 \pm 5 \text{ nA M}^{-1}$  for Ormosil-1,  $83 \pm 4 \text{ nA M}^{-1}$  for Ormosil-2, and  $137 \pm 5 \text{ nA M}^{-1}$  for Ormosil-3. The detection limits

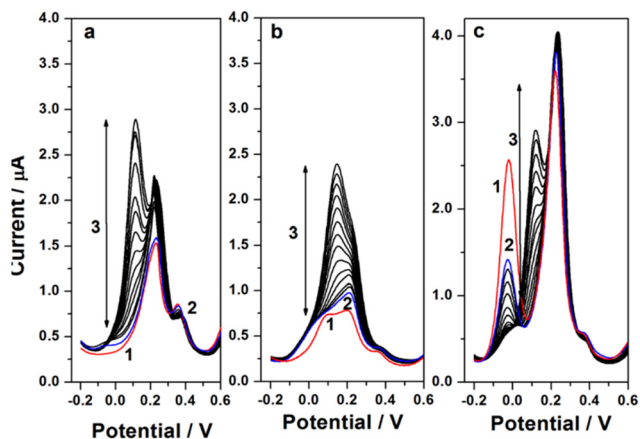


Fig. 8 Differential pulse voltammogram data from a polymer-modified electrode made with PI6CA containing (a) (1) TCNQ, (b) (1) Fc, and (c) (1) dmFc; (2) containing 1 mM AA, (3) repeated the addition of DA from 0.001 mM to 0.1 mM in 100 mM phosphate buffer (pH 7.4). Adopted with permission from ref. 23.

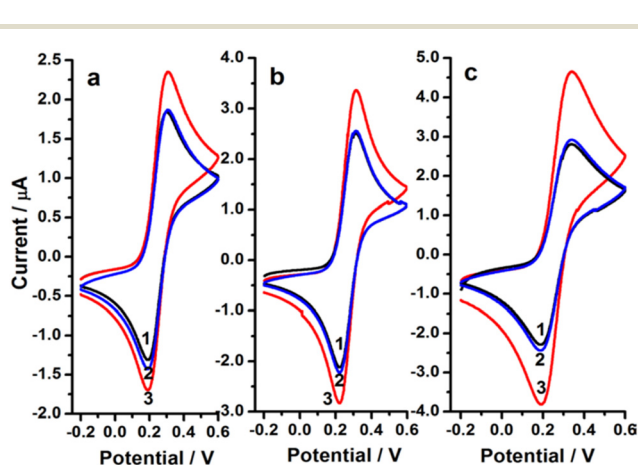


Fig. 9 Cyclic voltammograms of a polymer-modified electrode made with (a) (1) Ormosil®-1, (b) (1) Ormosil®-2, and (c) (1) Ormosil®-3; (2) containing 1 mM AA; (3) and 20 M DA in 100 mM phosphate buffer (pH 7.4) at a scan rate of  $0.01 \text{ V s}^{-1}$ . Adopted with permission from ref. 23.



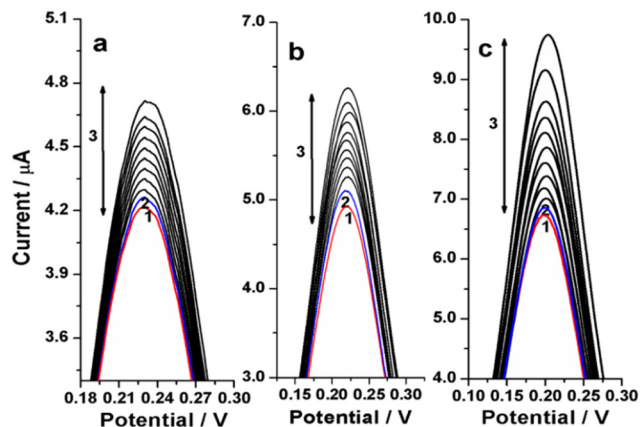


Fig. 10 Differential pulse voltammogram data from Ormosil@-1 (a), Ormosil@-2 (b), and Ormosil@-3 (c) film made with PI6CA containing (a) TCNQ, (b) Fc and (c) dmFc; (2) containing 1 mM AA and (3) subsequent additions of DA between 0.001–0.1 mM in 0.1 M phosphate buffer (pH 7.4). Adopted with permission from ref. 23.

were 340 nM for Ormosil-1, 200 nM for Ormosil-2, and 140 nM for Ormosil-3,<sup>17,22</sup> confirming the role of AuNPs in the electrochemical sensing of DA.

Parvin *et al.* doped CPs with semiconductor materials such as zinc oxide (ZnO) nanoparticles, which complement their properties by improving the electrical conducting behavior and reducing the band gap of the conductive PIN/ZnO composites.<sup>36</sup> An exfoliated molybdenum disulfide-based binary composite of PIN/MoS<sub>2</sub> was produced using solutions of indole monomers in the presence of ammonium phosphate (APS) by Choudhary *et al.*<sup>37</sup> Similarly, Raj *et al.* developed a PIN film electrodeposited with Co<sub>3</sub>O<sub>4</sub> with capacitive properties that was used for supercapacitor applications.<sup>38</sup> Zhou *et al.* fabricated bamboo-shaped *in situ* polymerized PIN/V<sub>2</sub>O<sub>5</sub> nanostructured composites with a large surface area, which acted as a potential ion exchanger in column chromatography.<sup>39,40</sup> Zhou *et al.* described the fabrication of carbon nanotube templated polycarbazole-based conjugated microporous polymeric membranes with excellent rheological properties and homogeneous pore sizes to enable the solvent to flow through; this structure exhibited a molecular sieve-like character.<sup>41</sup> Joshi *et al.* reported the design of PIN-nanocomposite (PNCs) hybrid electrodes using nanoscale tungsten carbide for selective and sensitive sensing of chlorpyrifos (CHL) *via* square-wave voltammetry.<sup>42</sup> Moon *et al.* reviewed the use of CP-based electrochemical sensors for neurotransmitters,<sup>43</sup> in which the electrode tip was applied to a human serum sample and showed excellent reproducibility.

### 3.3 Self-assembling polyindole–siloxane nanofluids and their role in electrochemical design

The presence of Si–O–Si linkage in a polymeric domain made from organosilane has been commonly referred to as siloxane; this material has been utilized for many biomedical

applications. For example, active surfaces have been demonstrated for antibody immobilization with superhydrophobic properties.<sup>57,59,65–67</sup> It has been shown that combining conductive polymer–siloxane copolymer nanocomposites and silicone-insulating polymers results in thin-layered structures with potential use in simple single-poled electrode designs;<sup>68</sup> these structures may possess high stability for *in vitro* testing. Siloxane was utilized in a single-contact prototype nerve cuff electrode;<sup>68</sup> this prototype involved processing peripheral nerve-stimulating electrodes out of conductive elastomers. When a siloxane–PIN sol is generated in a volatile solvent, the resulting fluid can be utilized for the fabrication of self-assembled thin films. A direct synthetic route that yields colloidal siloxane–PIN within a volatile organic solvent would allow for straightforward fabrication of thin membranes for a variety of applications, including medical device applications involving gas exchange (*e.g.*, soft contact lenses and artificial skin). Membranes derived from siloxane polymers may exhibit enhanced selectivity by integrating siloxane–PIN with a noble metal nanoparticle suspension.<sup>18,19</sup> This class of materials can exhibit unusual optical, electrical, mechanical, and thermal properties, which are attributed to the nanoparticles; for example, a variety of applications have been described for these materials when combined with silver nanoparticles.<sup>20,69</sup>

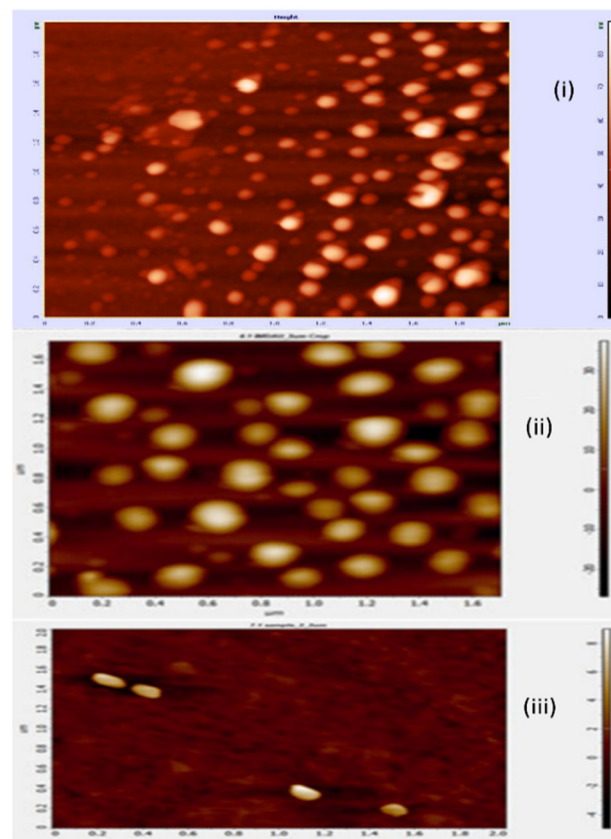


Fig. 11 AFM images of siloxane–AuNP sol (i), PIN–AuNPs sol (ii), and (iii) siloxane–PIN–AuNP–gold nanofluids.





Siloxane–PIN–AuNPs eliminate the presence of the scattering phenomenon and can be used for the processing of transparent and strong coatings, films, and membranes. The selection of an appropriate volatile solvent may allow for specific interactions between the siloxane polymer and the conducting polymer nanoparticles in a homogeneous hybrid suspension; this material is referred to as siloxane–PIN–nanoparticle nanofluid. The Lewis base character of functional organotrialkoxysilane (e.g., 3-aminopropyltrimethoxysilane (3-APTMS)), an imine derivative of siloxane, and an indole monomer has been noted to support the reduction of gold cations within acetone.<sup>17,18</sup> It should be noted that the Lewis acid–base adduct of the indole monomers and gold cations allows for the formation of PIN–AuNP–siloxane nanofluids. Fig. 11 (i) shows siloxane–gold nanoparticles, (ii) shows a self-assembly process that results in a polymeric nanofluid, and (iii) shows siloxane–PIN–AuNP membranes.<sup>17</sup> These membranes have been used to fabricate potentiometric ion sensors for cations and anions.<sup>17,18</sup> Nanofluids enable the processing of all-solid-state reference electrodes and ion-selective electrodes with specific nanofluid compositions in the presence of suitable reagents.<sup>17,18</sup> The electrochemical performance of a siloxane–AuNP film-modified electrode was examined in 5 mM potassium ferricyanide solution;<sup>59</sup> the electrochemistry of the as-prepared electrode in successive cycles using the same scan rate resulted in the accumulation of  $\text{Fe}(\text{CN})_6^{3-/4-}$  within the pores features of the film (Fig. 12) owing to the favorable electrostatic interactions that took place between the negatively charged  $\text{Fe}(\text{CN})_6^{3-/4-}$  probe and the positively charged siloxane matrix. The presence of AuNPs supports effective charge transfer; additional studies on this phenomenon are needed.

#### 4. Application of PIN and its nanocomposites in sensing

Among CPs, PIN can be cost-effectively synthesized on a large scale using either electrochemical methods or

chemical methods. These materials have been utilized in various technological applications owing to their unique properties, such as tunable bandgap values, surface tension, optical response, electronic conductivity, ionic conductivity, thermal stability, environmental stability, biocompatibility, and electrochemical properties. Researchers have also explored the impact of nanoparticle-induced modifications of PIN in terms of their electronic, magnetic, and optical properties. However, the main challenge in utilizing these conducting polymers for supercapacitors, thin-film transistors, electrochromic displays, organic LEDs, sensors, and environmental remediation is tailoring them for appropriate electrical conductivity, mechanical properties, and suitable fabrication procedures. PIN and their nanocomposites have numerous applications (Fig. 2);<sup>6</sup> compared to other materials, PIN and nanocomposites containing PIN possess numerous benefits for sensing and environmental remediation applications. The key characteristics exhibited by CPs and nanocomposites under an applied potential include electrocatalytic reduction and oxidation as well as pollutant uptake and release.<sup>6</sup>

The participation of the hydroxyl groups and amino groups connected to the polymer backbone of the PIN, as well as their surface roughness, facilitates the adsorption of pollutants. Ions of toxic metals are able to bond to  $\pi$ -electrons on the backbone of the polymers, leading to strong interactions. In photocatalysis, PIN can serve as a sensitizer that aids a metal oxide photocatalyst and supports the degradation of specific dyes under visible light exposure. PINs exhibit a high level of charge-carrier mobility; nanocomposites can be prepared that support effective charge separation when photodegradation of pollutants takes place under exposure to simulated sunlight. Additionally, conventional biosensors face challenges, such as a high detection limit, slow response, and low selectivity; these limitations present opportunities for the use of nanobiosensors that are based on CP nanomaterials. CPs

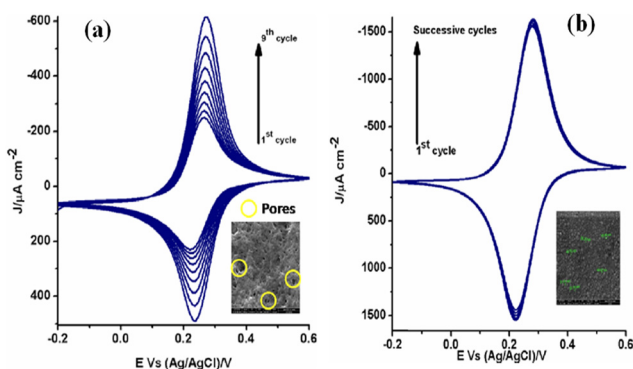


Fig. 12 (a) Cyclic voltammogram of siloxane–Au<sub>sim</sub> NPs showing increasing current trend at a scan rate of 10 mV s<sup>-1</sup> (b) cyclic voltammogram of Au@siloxane<sub>homo</sub> current with successive cycles at a scan rate of 10 mV s<sup>-1</sup>. Inset showing TEM micrographs of siloxane immobilized AuNPs (siloxane–Au<sub>sim</sub> NPs).

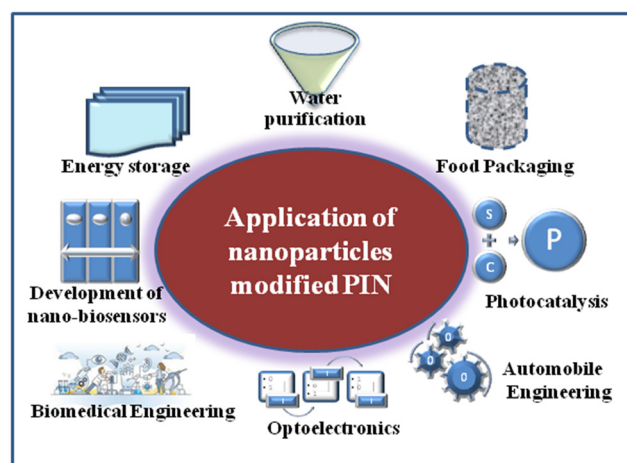


Chart 2 Multifunctional role of polyindole polymer composites.



possess unique properties that enable the customization of nanobiosensors to meet specific needs (Chart 2).

The use of PIN as a sensor is advantageous for material scientists because of its high sensitivity, biocompatibility, rapid response time, economical synthesis process, and rapid charge transfer characteristics with various target analytes at room temperature.<sup>70,71</sup> When the material is exposed to an analyte, analyte–material interactions may influence various properties such as mass, electrical conductivity, work function, color, solvation effects, backbone conformations, and the attraction of dopant counter ions or electrons in the CP films.<sup>70,72</sup> These changes result in the production of electrical signals that allow CPs to function as chemical sensors.<sup>72</sup> One example of this method is the quantification of the concentration of the analyte in solution or gas.<sup>72</sup> Among the various types of chemical sensors, electrochemical sensors have gained significant attention owing to their accuracy, ease of manufacture, and ease in terms of analysis of results.<sup>73</sup> The critical parameters associated with the evaluation of a sensor include its selectivity, sensitivity, response rate, and stability.<sup>74</sup> The sensitivity of a CP-based sensor is dependent on factors such as its specific surface area, device configuration, catalytic activity, and conductivity.<sup>74</sup> Various strategies to customize CPs for electrochemical sensor applications have been reported in the literature. The optimal choice of experimental conditions, including the supporting electrolyte, solvent, dopant, pH, and amount of charge passed, allows for the modulation of the binding properties, viscoelastic properties, porosity, thickness, and morphology of the CP films.<sup>75</sup>

The response of certain sensors is limited by their linear range; interference can take place with both the ionic species and the redox species that are present in the system. By hybridizing with carbon nanotubes, graphene, metal, metal oxide nanoparticles, and biological materials, these issues can be addressed by enhancing the molecular interactions, transport performance, and electrocatalytic reactivity.<sup>76</sup> PIN sensors modified with nanomaterials have demonstrated significant improvements in terms of versatility, sensitivity, and selectivity because nanomaterials possess unique optical, catalytic, electrical, and functional characteristics. These sensors are widely used for measuring and amplifying signals for various applications, such as the environmental detection of trace metals, medical diagnosis, and food monitoring. Approaches such as doping, affinity interactions, covalent attachment, and physical adsorption are commonly used to include recognition elements within a conducting polymer matrix.<sup>6,76</sup>

Among these approaches, doping is the most widely used method in electroanalysis because of its reproducibility in creating sensors for detecting multiple targets. Unlike traditional chemical sensors, biosensors involve the immobilization of enzymes, oligonucleotides, aptamers, antibodies/antigens, and other types of biological recognition agents within conducting polymers, which can detect the presence of an analyte<sup>77</sup> (Fig. 13). There are five main

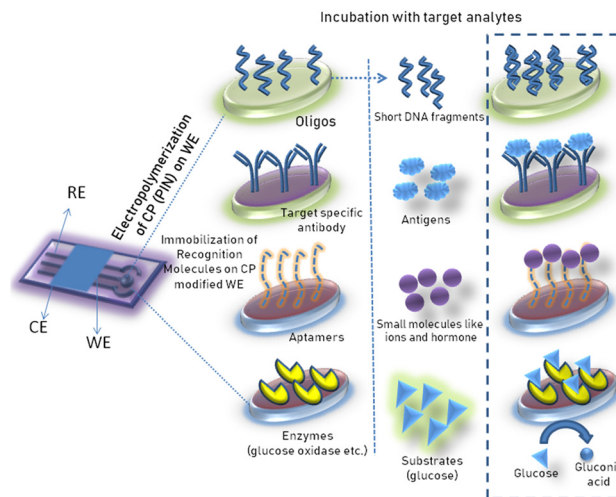


Fig. 13 CP based biosensors. Immobilization of recognition elements and binding of target molecules.

categories of biorecognition techniques based on the transduction mechanism: resonant biosensors, thermal detection biosensors, optical detection biosensors, ion-sensitive field-effect transistor-based biosensors, and electrochemical biosensors.<sup>78</sup> Numerous electrochemical biosensors based on PIN and PPY films have been prepared for detecting various analytes such as dopamine, cholesterol, hydrogen peroxide, glucose, cysteine, hydrazine, and kanamycin.<sup>78</sup> Advances in PIN-modified materials for detecting different chemical substances in liquid and gas forms are presented in Table 1. The biological characteristics of PIN can be improved by modification with nanomaterials; these conducting polymers can be used in tissue engineering, drug delivery, bioelectronics, and biorecognition applications. PIN-based materials are extensively used for detecting various chemical species through electrical detection at electrode interfaces *via* impedimetric, amperometric, potentiometric, chemoresistance, electrochemical luminescence, field-effect transistor, and photoelectrochemical approaches that react swiftly to changes in the voltage, current, and resistance.<sup>79</sup> In addition, fluorescence sensors have gained considerable attention for sensing applications.<sup>80</sup> Self-healing, stimuli-responsive, and conductive hydrogels of PIN have been demonstrated that exhibit metal-like electrical conductivity and hydrogel-like flexible mechanical properties.<sup>81–83</sup> Nie *et al.*<sup>84</sup> developed a nanostructured composite material composed of poly(indole-6-carboxylic acid) (PICA) and carboxylic group-ended multiwalled carbon nanotubes (MWNTs). This material was electrosynthesized with an indole-6-carboxylic acid (ICA) monomer and MWNTs using a single step, with the MWNTs serving as the supporting electrolytes. The researchers utilized this composite material to create an electrochemical sensor for the detection of target DNA related to the hepatitis B virus (HBV) (Fig. 14).<sup>84</sup> Other materials, including 3D nanostructures and dendrimers, can be used for promoting selectivity and enhancing mass transfer. PIN structures with



**Table 1** CP (PIN) based nanocomposite fabricated biosensor for the detection of different analytes. Adapted with permission<sup>6</sup> © the authors

Biosensor composition	Analyte	Detection limit	Linear range	Ref.
PiN5-COOH/ZnS	D-Amino acid	0.001 mM	0.001 to 2.0 mM	85
MWNT-PIN6-COOH	DNA	2.0 fmol L <sup>-1</sup>	1.0 × 10 <sup>-14</sup> to 5.0 × 10 <sup>-12</sup> mol L <sup>-1</sup>	84
PIN6-COOH/ODN	DNA	5.79 pmol L <sup>-1</sup>	3.5 × 10 <sup>-10</sup> to 2.0 × 10 <sup>-8</sup> mol L <sup>-1</sup>	86
Poly(5-formylindole)/ODN	Ramos cells	300 cells per mL	500 to 1.0 × 10 <sup>5</sup> cells per mL	87
PiN-5-COOH/MWCNTs-COOH	Alpha-fetoprotein (α-FP)	0.33 pg mL <sup>-1</sup>	0.001 ng mL <sup>-1</sup> to 100 ng mL <sup>-1</sup>	88
QDs/PICA-MWNT	Alpha-fetoprotein (α-FP)	0.4 pg mL <sup>-1</sup>	0.002 to 2000 ng mL <sup>-1</sup>	89
AuNP/GQDs-PEI-GO (PICA/FGNs as substrate for fabrication)	Prostate-specific antigen (PSA)	0.44 pg mL <sup>-1</sup>	0.001 ng mL <sup>-1</sup> to 100 ng mL <sup>-1</sup>	90
Au-PiN-RGO	Caffeine	0.26 μM	0.8 to 40 μM	91
PICA/F-Au nanocomposite	Aflatoxin B1 (AFB1)	0.00375 ng mL <sup>-1</sup>	0.01 to 100 ng mL <sup>-1</sup>	92
PiN/GQDs@MIPs	Dopamine	1 × 10 <sup>-10</sup> M	5 × 10 <sup>-10</sup> to 1.2 × 10 <sup>-6</sup> M	93
Polyindole-siloxane-gold nanofluid	Chloride ion	—	—	18
PiN/rGO/Ag	Ascorbic acid	1.5 μM	0.2 to 1 mM	94
dPiN-MWCNT	Acetylcholine	1.27 nM	10 <sup>-5</sup> to 10 <sup>-2</sup> M	95
MXene-dPiN and MWCNT-dPiN	Glucose	0.115 mM	2.5 to 10 mM	96
GCE/AuNPs-ERGO/PiN-5-COOH	H <sub>2</sub> O <sub>2</sub>	0.008 μmol L <sup>-1</sup>	0.025 to 750 μmol L <sup>-1</sup>	97
(PiN)/Mn <sub>2</sub> O <sub>3</sub> nanocomposite and PiN/Mn <sub>2</sub> O <sub>3</sub> /polyaniline (PANI)	Cd <sup>2+</sup> and Pb <sup>2+</sup>	10.72 L <sup>-1</sup> for Pb <sup>2+</sup> and 9.85 μg L <sup>-1</sup> for Cd <sup>2+</sup> for PiN/Mn <sub>2</sub> O <sub>3</sub> nanocomposite; 0.05 L <sup>-1</sup> for Pb <sup>2+</sup> and 0.02 μg L <sup>-1</sup> for Cd <sup>2+</sup> for PiN/Mn <sub>2</sub> O <sub>3</sub> /polyaniline (PANI)	1 to 200 μg L <sup>-1</sup> for PiN/Mn <sub>2</sub> O <sub>3</sub> nanocomposite and 0.05 to 450 μg L <sup>-1</sup> for PiN/Mn <sub>2</sub> O <sub>3</sub> /polyaniline (PANI)	98
PiN/rGO/Ag	Ascorbic acid	1.5 μM	0.2 to 1 mM	69
APiN/P-g-C <sub>3</sub> N <sub>4</sub>	Serum amyloid A (SAA)	5 ng mL <sup>-1</sup>	5 ng mL <sup>-1</sup> to 500 μg mL <sup>-1</sup>	99
PI-W <sub>2</sub> O <sub>7</sub> NCs	Cd(II)	1.072 ppb	—	100

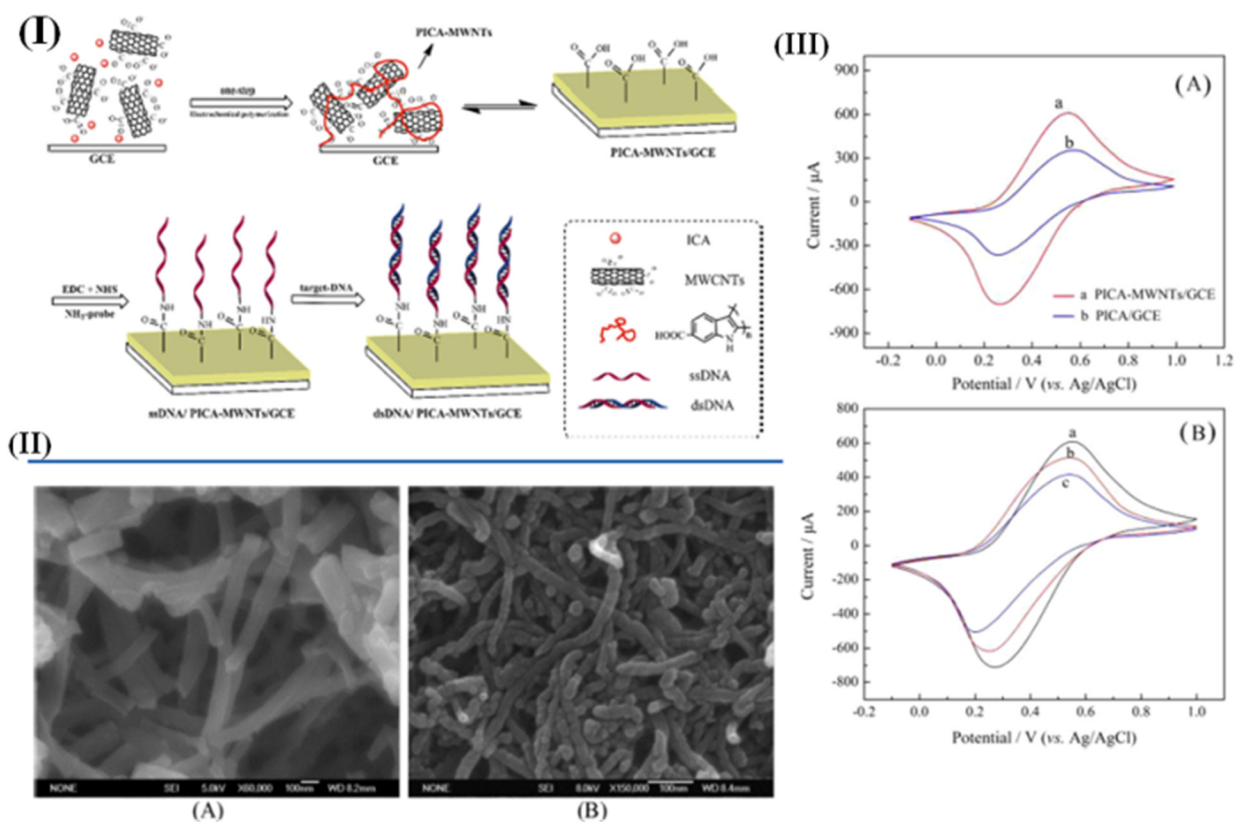


**Fig. 14** (I) Preparations of PICA-MWNT composite material and the corresponding conceptual scheme for label-free DNA detection, (II) SEM of PICA film (A) and PICA-MWNT composite film (B) deposited on GCE and (III) CVs of (A) PICA-MWNT (a) and pure PICA film (b); (B) PICA-MWNT (a), ssDNA/PICA-MWNT (b), and dsDNA/PICA-MWNT (c) in NaAc-HAc buffer (pH = 6.5, 0.1 mol L<sup>-1</sup> NaCl). Scan rate: 100 mV s<sup>-1</sup>. Reproduced with permission,<sup>84</sup> © ACS 2012.



nanobelts, nanorods, nanowires, and nanofiber morphologies offer a higher surface area, enhanced conductivity, and continuous charge transfer compared to nanospheres. Future research efforts are anticipated to focus on utilizing PIN structures in both virgin forms and composite forms for the detection and removal of pollutants.

## 5. Conclusions

Conducting polymers have attracted significant attention because of their potential role in the development of multidisciplinary sensing components. Heterocyclic conjugated organic molecules, specifically indole and its derivatives, exhibit functionality related to electrochemically controlled susceptibility, specifically the ability to exhibit electroactivity in different compatible solvent media. These characteristics have facilitated the development of materials from excitable hydrophobic materials to water-soluble polyindoles, including self-assembling nanofluids, for a variety of applications. Potential applications of these materials include rechargeable batteries and supercapacitors, silicate-polyindole-modified electrodes, polyindole-nanomaterial-modified electrodes, and self-assembling nanofluids. Advances in these materials have proven to be highly favorable for biological applications owing to their high level of biocompatibility. To realize the potential of CPs in certain areas (e.g., n-type bioelectronics), additional assessments in terms of manufacturability and application-specific performance are needed.

## Data availability

This review article does not contain new data that have been generated or analyzed by the author. All of the data referenced in this paper are available in the original publications that are cited in the reference list.

## Author contributions

PCP and AKT contributed equally to this study PCP, AKT, and RJN wrote and edited the manuscript. All authors have read and agreed to the publication of this manuscript.

## Conflicts of interest

There are no conflicts to declare.

## Acknowledgements

No external or internal funding source to declare.

## References

- B. B. Berkes, A. S. Bandarenka and G. Inzelt, *J. Phys. Chem. C*, 2015, **119**, 1996–2003.
- N. Mkhize, K. Murugappan, M. R. Castell and H. Bhaskaran, *J. Mater. Chem. C*, 2021, **9**, 4591–4596.
- N. Ö. Alayunt and C. Soykan, *Microsc. Res. Tech.*, 2021, **84**, 326–336.
- F. Tassinari, D. Amsallem, B. P. Bloom, Y. Lu, A. Bedi, D. H. Waldeck, O. Gidron and R. Naaman, *J. Phys. Chem. C*, 2020, **124**, 20974–20980.
- R. J. Waltman, A. F. Diaz and J. Bargon, *J. Phys. Chem.*, 1984, **88**, 4343–4346.
- A. Thadathil, H. Pradeep, D. Joshy, Y. A. Ismail and P. Periyat, *Mater. Adv.*, 2022, **3**, 2990–3022.
- P. C. Pandey, *J. Chem. Soc., Faraday Trans. 1*, 1988, **84**, 2259–2265.
- P. C. Pandey and R. Prakash, *J. Electrochem. Soc.*, 1998, **145**, 999.
- K. M. Choi, C. Y. Kim and K. H. Kim, *J. Phys. Chem.*, 1992, **96**, 3782–3788.
- G. Zotti, S. Zecchin, G. Schiavon, R. Seraglia, A. Berlin and A. Canavesi, *Chem. Mater.*, 1994, **6**, 1742–1748.
- H. Talbi, E. B. Maarouf, B. Humbert, M. Alnot, J. J. Ehrhardt, J. Ghanbaja and D. Billaud, *J. Phys. Chem. Solids*, 1996, **57**, 1145–1151.
- P. C. Pandey and R. Prakash, *J. Electrochem. Soc.*, 1998, **145**, 4103.
- P. C. Pandey and R. Prakash, *Sens. Actuators, B*, 1998, **46**, 61–65.
- P. C. Pandey, R. Prakash, G. Singh, I. Tiwari and V. S. Tripathi, *J. Appl. Polym. Sci.*, 2000, **75**, 1749–1759.
- P. C. Pandey, G. Singh, H. S. Sharma and S. K. Aggarwal, *BARC*, 2009, vol. 404, p. 309, [https://barc.gov.in/barc\\_nl/2009/200910.pdf](https://barc.gov.in/barc_nl/2009/200910.pdf).
- P. C. Pandey, D. S. Chauhan and V. Singh, *Electrochim. Acta*, 2009, **54**, 2266–2270.
- P. C. Pandey, D. S. Chauhan and V. Singh, *Mater. Sci. Eng., C*, 2012, **32**, 1–11.
- P. C. Pandey, N. Katyal, G. Pandey and R. J. Narayan, *MRS Commun.*, 2020, **10**, 482–486.
- P. C. Pandey and G. Pandey, *Indian Pat.*, 343403, 2020.
- P. C. Pandey and G. Pandey, *Indian Pat.*, 202011014527, 2020.
- P. C. Pandey, G. Pandey and R. J. Narayan, *Med. Devices Sens.*, 2020, e10110.
- P. C. Pandey, D. S. Chauhan and V. Singh, *Front. Biosci., Elite Ed.*, 2013, **5**, 622–642.
- V. Singh, D. S. Chauhan and P. C. Pandey, in *SENSORS, 2009 IEEE*, 2009, pp. 1140–1145.
- P. S. Abthagir, K. Dhanalakshmi and R. Saraswathi, *Synth. Met.*, 1998, **93**, 1–7.
- J. Xu, G. Nie, S. Zhang, X. Han, J. Hou and S. Pu, *J. Polym. Sci., Part A: Polym. Chem.*, 2005, **43**, 1444–1453.
- E. B. Maarouf, D. Billaud and E. Hannecart, *Mater. Res. Bull.*, 1994, **29**, 637–643.
- N. S. Wadatkar and S. A. Waghuley, *Egypt. J. Basic Appl. Sci.*, 2015, **2**, 19–24.
- B. Purty, R. B. Choudhary, A. Biswas and G. Udayabhanu, *Polym. Bull.*, 2019, **76**, 1619–1640.
- Q. Guo, J. Li, B. Zhang, G. Nie and D. Wang, *ACS Appl. Mater. Interfaces*, 2019, **11**, 6491–6501.
- D. Billaud, E. B. Maarouf and E. Hannecart, *Synth. Met.*, 1995, **69**, 571–572.



- 31 A. Eftekhari, L. Li and Y. Yang, *J. Power Sources*, 2017, **347**, 86–107.
- 32 J. G. Mackintosh, C. R. Redpath, A. C. Jones, P. R. Langridge-Smith and A. R. Mount, *J. Electroanal. Chem.*, 1995, **388**, 179–185.
- 33 I. Marriam, Y. Wang and M. Tebyetekerwa, *Energy Storage Mater.*, 2020, **33**, 336–359.
- 34 C. Zhu, G. Yang, H. Li, D. Du and Y. Lin, *Anal. Chem.*, 2015, **87**, 230–249.
- 35 N. Chauhan, J. Narang and U. Jain, *J. Exp. Nanosci.*, 2016, **11**, 111–122.
- 36 M. H. Parvin, M. Pirnia and J. Arjomandi, *Electrochim. Acta*, 2015, **185**, 276–287.
- 37 R. B. Choudhary, M. Majumder and A. K. Thakur, *ChemistrySelect*, 2019, **4**, 6906–6912.
- 38 R. P. Raj, P. Ragupathy and S. Mohan, *J. Mater. Chem. A*, 2015, **3**, 24338–24348.
- 39 X. Zhou, Q. Chen, A. Wang, J. Xu, S. Wu and J. Shen, *ACS Appl. Mater. Interfaces*, 2016, **8**, 3776–3783.
- 40 L. Zou, X. Duan, W. Zhou, H. Zhang, S. Chen, J. Chai, X. Liu, L. Shen, J. Xu and G. Zhang, *J. Mater. Sci.: Mater. Electron.*, 2019, **30**, 7850–7857.
- 41 Z. Zhou, X. Li, D. Guo, D. B. Shinde, D. Lu, L. Chen, X. Liu, L. Cao, A. M. Aboalsaud, Y. Hu and Z. Lai, *Nat. Commun.*, 2020, **11**, 5323.
- 42 P. Joshi, S. Mehtab, M. G. Zaidi, T. Tyagi and A. Bisht, *J. Nanostruct. Chem.*, 2020, **10**, 33–45.
- 43 J. M. Moon, N. Thapliyal, K. K. Hussain, R. N. Goyal and Y. B. Shim, *Biosens. Bioelectron.*, 2018, **102**, 540–552.
- 44 A. Palma-Cando, I. Rendón-Enríquez, M. Tausch and U. Scherf, *Nanomaterials*, 2019, **9**, 1125.
- 45 Z. Chen, E. Villani and S. Inagi, *Curr. Opin. Electrochem.*, 2021, **28**, 100702.
- 46 K. Namsheer and C. S. Rout, *RSC Adv.*, 2021, **11**, 5659–5697.
- 47 L. Q. Flagg, C. G. Bischak, J. W. Onorato, R. B. Rashid, C. K. Luscombe and D. S. Ginger, *J. Am. Chem. Soc.*, 2019, **141**, 4345–4354.
- 48 P. Audebert and F. Miomandre, Electrochemistry of conducting polymers, in *Conjugated Polymers*, CRC Press, 2019, pp. 161–199.
- 49 M. J. Lefferts, L. H. Humphreys, N. Mai, K. Murugappan, B. I. Armitage, J. F. Pons and M. R. Castell, *Analyst*, 2021, **146**, 2186–2193.
- 50 R. B. Choudhary, S. Ansari and M. Majumder, *Renewable Sustainable Energy Rev.*, 2021, **145**, 110854.
- 51 J. S. Noori, J. Mortensen and A. Geto, *Sensors*, 2021, **21**, 393.
- 52 J. G. Wu, J. H. Chen, K. T. Liu and S. C. Luo, *ACS Appl. Mater. Interfaces*, 2019, **11**, 21294–21307.
- 53 R. Wang, W. Zhou, K. Lin, F. Jiang, Z. Wang, J. Xu, Y. Zhang, A. Liang, G. Nie and X. Duan, *Electrochim. Acta*, 2020, **349**, 136410.
- 54 H. Mudila, P. Prasher, M. Kumar, A. Kumar, M. G. Zaidi and A. Kumar, *Mater. Renewable Sustainable Energy*, 2019, **8**, 1–9.
- 55 R. Yue, F. Jiang, Y. Du, J. Xu and P. Yang, *Electrochim. Acta*, 2012, **77**, 29–38.
- 56 J. Heinze, B. A. Frontana-Urbe and S. Ludwigs, *Chem. Rev.*, 2010, **110**, 4724–4771.
- 57 E. Pouget, J. Tonnar, P. Lucas, P. Lacroix-Desmazes, F. Ganachaud and B. Boutevin, *Chem. Rev.*, 2010, **110**, 1233–1277.
- 58 F. Abbasi, H. Mirzadeh and A.-A. Katbab, *Polym. Int.*, 2001, **50**, 1279–1287.
- 59 P. C. Pandey, G. Pandey and A. Walcarius, *Mater. Sci. Eng., C*, 2017, **79**, 45–54.
- 60 K. M. Choi, C. Y. Kim and K. H. Kim, *J. Phys. Chem.*, 1992, **96**, 3782–3788.
- 61 M. Faraz, M. Shakir and N. Khare, *New J. Chem.*, 2017, **41**, 5784–5793.
- 62 K. Phasuksom, W. Prissanaroon-Ouajai and A. Sirivat, *RSC Adv.*, 2020, **10**, 15206–15220.
- 63 G. Wang, A. Morrin, M. Li, N. Liu and X. Luo, *J. Mater. Chem. B*, 2018, **6**, 4173–4190.
- 64 R. Ciriminna, A. Fidalgo, V. Pandarus, F. Beland, L. M. Ilharco and M. Pagliaro, *Chem. Rev.*, 2013, **113**, 6592–6620.
- 65 P. C. Pandey, S. Upadhyay and H. C. Pathak, *Electroanalysis*, 1999, **11**, 59–64.
- 66 P. C. Pandey and B. Singh, *Biosens. Bioelectron.*, 2008, **24**, 842–848.
- 67 G. R. Artus, S. Jung, J. Zimmermann, H. P. Gautschi, K. Marquardt and S. Seeger, *Adv. Mater.*, 2006, **18**, 2758–2762.
- 68 F. Keohan, X. F. Wei, A. Wongsarnpigoon, E. Lazaro, J. E. Darga and W. M. Grill, *J. Biomater. Sci., Polym. Ed.*, 2007, **18**, 1057–1073.
- 69 S. Younis, F. Liaqat, A. Jabeen and S. Ahmed, *Mater. Chem. Phys.*, 2024, **316**, 129113.
- 70 Y. Wang, A. Liu, Y. Han and T. Li, *Polym. Int.*, 2020, **69**, 7–17.
- 71 M. Das and S. Roy, *Mater. Sci. Semicond. Process.*, 2021, **121**, 105332.
- 72 Q. Ameer and S. B. Adeloju, *Sens. Actuators, B*, 2005, **106**, 541–552.
- 73 A. Walcarius, S. D. Minter, J. Wang, Y. Lin and A. Merkoçi, *J. Mater. Chem. B*, 2013, **1**, 4878–4908.
- 74 Q. Zhou and G. Shi, *J. Am. Chem. Soc.*, 2016, **138**, 2868–2876.
- 75 G. Inzelt, *Conducting polymers: a new era in electrochemistry*, Springer Science & Business Media, 2012.
- 76 N. Aydemir, J. Malmström and J. Travas-Sejdic, *Phys. Chem. Chem. Phys.*, 2016, **18**, 8264–8277.
- 77 A. Al-Ahmed, H. M. Bahaidarah and M. A. Mazumder, *Adv. Mater. Res.*, 2013, **810**, 173–216.
- 78 M. Naseri, L. Fotouhi and A. Ehsani, *Chem. Rec.*, 2018, **18**, 599–618.
- 79 R. Gangopadhyay and A. De, *Chem. Mater.*, 2000, **12**, 608–622.
- 80 M. Faraz, A. Abbasi, F. K. Naqvi, N. Khare, R. Prasad, I. Barman and R. Pandey, *Sens. Actuators, B*, 2018, **269**, 195–202.



- 81 Z. Deng, R. Yu and B. Guo, *Mater. Chem. Front.*, 2021, **5**, 2092–2123.
- 82 Z. Deng, T. Hu, Q. Lei, J. He, P. X. Ma and B. Guo, *ACS Appl. Mater. Interfaces*, 2019, **11**, 6796–6808.
- 83 Z. Deng, H. Wang, P. X. Ma and B. Guo, *Nanoscale*, 2020, **12**, 1224–1246.
- 84 G. Nie, Z. Bai, J. Chen and W. Yu, *ACS Macro Lett.*, 2012, **1**, 1304–1307.
- 85 S. Lata, B. Batra and C. S. Pundir, *Process Biochem.*, 2012, **47**, 2131–2138.
- 86 G. Nie, Y. Zhang, Q. Guo and S. Zhang, *Sens. Actuators, B*, 2009, **139**, 592–597.
- 87 G. Nie, Z. Bai, W. Yu and J. Chen, *Biomacromolecules*, 2013, **14**, 834–840.
- 88 T. Yang, X. Ren, M. Yang, X. Li, K. He, A. Rao, Y. Wan, H. Yang, S. Wang and Z. Luo, *Biosens. Bioelectron.*, 2019, **141**, 111406.
- 89 G. Nie, C. Li, L. Zhang and L. Wang, *J. Mater. Chem. B*, 2014, **2**, 8321–8328.
- 90 C. Yang, Q. Guo, Y. Lu, B. Zhang and G. Nie, *Sens. Actuators, B*, 2020, **303**, 127246.
- 91 R. Li, L. Yao, Z. Wang, W. Lv, W. Wang, F. Kong and W. Wang, *J. Electrochem. Soc.*, 2019, **166**, B212.
- 92 Y. Lu, X. Zhao, Y. Tian, Q. Guo, C. Li and G. Nie, *Microchem. J.*, 2020, **157**, 104959.
- 93 X. Zhou, A. Wang, C. Yu, S. Wu and J. Shen, *ACS Appl. Mater. Interfaces*, 2015, **7**, 11741–11747.
- 94 S. Younis, F. Liaqat, A. Jabeen and S. Ahmed, *Mater. Chem. Phys.*, 2024, **316**, 129113.
- 95 K. Phasuksom, N. Thongwattana, N. Ariyasajjamongkol and A. Sirivat, *J. Electroanal. Chem.*, 2024, **964**, 118337.
- 96 K. Phasuksom, N. Ariyasajjamongkol and A. Sirivat, *Heliyon*, 2024, **10**(2), e24346.
- 97 G. Aydoğdu Tığ and B. Zeybek, *Electroanalysis*, 2023, **35**, e202200064.
- 98 A. Yousefi, H. Aghaie, M. Giahi and L. Maleknia, *Chem. Pap.*, 2023, **77**, 733–743.
- 99 V. Nirbhaya, R. Chandra and S. Kumar, *Colloids Surf., B*, 2023, **230**, 113504.
- 100 F. Mashkoo, M. Shoeb, A. H. Anwer, I. Hasan, S. S. Baek and C. Jeong, *J. Environ. Chem. Eng.*, 2023, **11**, 111460.

